arXiv:cond-mat/0406309v1 [cond-mat.other] 14 Jun 2004

Effect of strain on the magnetic and transport properties of the composite manganites, $La_{2/3}Ca_{1/3}MnO_3$/yttria-stabilized zirconia

Wei Liu[1], Chinping Chen[1*], Xinfeng Wang[1], Jun Zhao[1], Xiangyu Xu[1], Jun Xu[1,2], and Shousheng Yan[1]
(1) Department of Physics and State Key Lab for Mesoscopic Physics, Peking University, Beijing 100871, P. R. China
(2) Electron microscopy laboratory, Peking University, Beijing 100871, P. R. China

The magnetic and transport properties have been investigated for the composite polycrystalline manganites, (1-x)$La_{2/3}Ca_{1/3}MnO_3$/(x)yttria-stabilized zirconia ((1-x)LCMO/(x)YSZ), at various YSZ fractions, x, ranging from 0 % to 15 %. The ac magnetic susceptibility, $\chi(T)$, DC magnetization, $M(T)$, temperature dependent resistivity, $\rho(T)$ and thermoelectric power (TEP), $S(T)$, have been measured. It was found, surprisingly, that a TEP peak showed up in the magnetic transition region for the sample with the x even as little as 0.75 %. The magnetic transition temperature reaches the minimum value as x increases from 0 % to 4.5 % and goes up as x increases further. Several possible factors such as the effect of strain, the finite size effect, and the effect of magnetic tunnelling coupling, *etc.*, in affecting the above physical properties of the composite manganites have been studied carefully. The strain induced by the YSZ/LCMO boundary layer (BL) was identified as the leading factor to account for the x dependence of these properties. It demonstrates that the effect of strain could be important in the bulk manganites as in the film sample.

I. INTRODUCTION

The perovskite manganites, $A_{1-y}B_yMnO_3$, in which A is for the rare earth trivalent cation and B for the alkaline divalent one, exhibit complicated phases at various temperatures and hole doping concentrations, y. Due to the important magnetic application potentials and fundamental research interests, tremendous activities in the physics community have focused in this area during the past decade. With an appropriate doping concentration y, an FM transition takes place at the Curie point, T_C, with the decreasing temperature. It is accompanied with the metal-insulator (MI) transition at T_P. A colossal magneto-resistance (CMR) slao occurs around this temperature. These properties can be explained with the double exchange (DE) mechanism,[1–4].

Recently, growing attentions have been focused on the effect of strain arising from the interface or surface states of the CMR thin film[5–7]. The variation of the magnetic transition temperature, T_C, was interpreted as attributed to the strain. However, it is usually difficult to separate the strain-induced effect from the finite size confinement one with the thin films[8–10]. On the other hand, the effect of strain is usually overlooked in the bulk samples. We would like to demonstrate that the effect of the BL strain with the polycrystalline composite manganites, (1-x)LCMO/(x)YSZ, is a very important factor for the variation of the physical properties such as T_C, the temperature dependent resistivity, $\rho(T)$, and the $S(T)$ behavior, *etc.*.

II. SAMPLE PREPARATION

A double-staged process was applied in preparing the LCMO/YSZ samples[11]. In the first stage, the LCMO nano-sized powder was produced by the sol-gel method and then sintered at 1300 ^oC for 10 hours to form crystals of about 20 μm. In the second stage, the thus-obtained LCMO powders were mixed with the YSZ powders of about 2 μm for the heat treatment at 1350 ^oC for another 10 hours. The X-ray diffraction (XRD) was performed by a Philip x' pert diffractometer using the Cu K_α line (1.54056 $\AA$). The XRD spectra are presented in Fig. 1. The YSZ phase was identified for the samples with x exceeding 4.5 %. The lattice constants of the LCMO phase remain unchanged within 0.001 $\AA$ for all of the YSZ mixing concentration, x. This indicates that, within the detection sensitivity of XRD, the bulk LCMO composition was not modified during the heat treatment due to any possible diffusion of ions from the YSZ composition. We have prepared the samples of LCMO annealed at 1400 ^oC without the mixing of YSZ as well. This would demonstrate the widely investigated disorder effect resulting from different annealing conditions.

The morphology of the sample was investigated by a scanning electron microscope (SEM) performed on the system of FEI STRATA DB235 focus ion beam (FIB) electron microscope. It revealed that at low mixing concentration, x < 4.5 %, the LCMO phase formed large cluster surrounded by a thin layer of YSZ component at a thickness of the order of 10 nm. The BL area increases while the cluster size of the LCMO phase decreases with the increasing YSZ fraction. The interconnecting paths between the adjacent LCMO clusters separated by the YSZ layers would reduce accordingly. On the other hand, at the mixing fraction, x, exceeding about 4.5 %, the YSZ phase forms cluster-like structure by itself. Thus, the BL area decreases correspondingly. This observation is consistent with the previous report[11]. Within the detection sensitivities of the XRD and SEM, no indication of the inter diffusion between the LCMO and the YSZ phases exists. The two phases, hence, form solid mixture with the existence of the BL strain in between. Since the YSZ

phase is insulating and non-magnetic. the LCMO/YSZ composites are, therefore, appropriate for the investigation of the magnetic and transport properties under the BL strain.

III. EXPERIMENT

The dc magnetization, $M(T)$, and ac magnetic susceptibility, $\chi(T) = \chi' + i\chi''$, were performed using Quantum Design PPMS and MPMS, respectively. The ac susceptibility measurement was carried out with the excitation field of 10 Oe at 113 Hz under a few Oe of dc background field. The applied field for the $M(T)$ measurement, including the field-cooled (FC) and zero-field-cooled (ZFC), is 50 Oe, while the field applied during the cooling stage before the FC measurement is 3000 Oe. The magnetic transition temperatures, $T_C(dc)$ and $T_C(ac)$, are obtained using the definition, dM/dT and $d\chi'/dT$. These two transition temperatures agree with each other well within a few Kelvin, as plotted in Fig. 2. Also plotted in the same figure are the metal-insulator (MI) transition temperature, T_P, determined by the $\rho(T)$ measurement, and the magnetic transition temperature width, ΔT, defined by the difference of temperatures at which $d\chi'/dT = 0$. The correlation of the T_C with the BL effect is apparent in the figure. The lowest T_C occurs at x = 4.5 %, corresponding to the minimum BL inferred from the SEM observation. In order to investigate the effect of thermal treatment on T_C, the sample of x = 0 annealed at 1400 ^oC was measured as well for the magnetic transition temperature, T_C. It is 260 K using the same maximum slope criteria described above. The depression of T_C down to about 245 K with the sample annealed at 1300 ^oC accounts for about 6 % effect. This is a well studied effect and is attributed to the disorder associated with the polycrystalline grain size distribution,[12,13].

The out-of-phase component, $\chi''(T)$, is shown in Fig. 3. Two characteristic dissipation features, the peak at high temperature, T_{DH}, and the bump at low temperature, T_{DL}, appear for each sample and are depicted in the inset of Fig. 3 as a function of the YSZ fraction, x. T_{DH} is lower than T_C by a few Kelvins. It is resulting from the energy dissipation process associated with the critical spin fluctuation near the FM phase transition. The x-dependence of T_{DH} is therefore similar to that of T_C. On the other hand, T_{DL} appears around 70 K for all of the samples, including the one with x = 0. This indicates that the LT bump is independent of the BL. In fact, similar bumps in $\chi''(T)$ at $T < T_C$ have been observed in many previous experiments, attributed to the magnetic inhomogeneity[14]. Hence, the x independence of T_{DL} is an indication that the characteristic crystalline grain size associated with the LCMO phase stays unaltered with the mixing of the YSZ component. The field-cooled (FC) and zero-field-cooled (ZFC) dc magnetization measurements on the chosen samples, x = 0 %, 1.25 %, 4.5 % and 15 %, were performed to investigate the magnetic inhomogeneity. Fig. 4 shows the normalized magnetization, M(T)/M_m, versus the reduced temperature, T/T_C, where M_m is the maximum magnetization occurring near the freezing temperature at which the FC and ZFC branches of the $M(T)$ curves diverge. There is no appreciable difference for the x = 0 % sample from the other ones, indicating that the magnetic disorder revealed by this measurement is ascribed to the polycrystalline grains, independent of the BL. This is of the same origin causing the LT bump in the $\chi''(T)$ measurements. Note that, there is no structure in the $M(T)$ curve or the in-phase component, $\chi'(T)$ (not shown here), at the temperature near the LT bump. It indicates that it is not resulting from a magnetic phase transition.

The $\rho(T)$ measurement was carried out from 80 K to 300 K in a home-made insert-probe by a standard 4-probe dc techniques using cold-pressed indium as the electrical contacts. The typical contact resistances is on the order of a few Ω with the applied current on the order of a few mA. The $\rho(T)$ curves are published in Fig. 1 by Liu *et al*[15]. In the region below T_C, the $\rho(T)$ behaviors are analyzed with the various scattering processes of the electrons by the function $\rho(T) = \rho_0 + AT^a + BT^b$, where a = 2 or 3/2, and b = 5 or 9/2. The maximum fitting range in temperature for a stable result is from the lowest temperature of the measurement to $T \sim 0.8\ T_C$. The AT^a term with a = 2 or 3/2 gives equally good fitting of the experimental data. The coefficient of the fitting, A, corresponding to a = 3/2 or 2 also exhibits identical x dependence. It is difficult to distinguish which of the following two processes is the more important one, the T^2 term for the electron-electron scattering or the $T^{3/2}$ term for the scattering of electrons by the disordered spin glass component[16]. The x dependence of this term is represented by the coefficient A, calculated using a = 2, versus x and plotted in Fig. 5. The variation with different samples is within a factor of 4. Similarly, an equally good fitting is obtained with the BT^b term using b = 5 for the electron-phonon scattering or b = 9/2 for the electron-magnon scattering within the framework of DE mechanism[17]. Since the B-variation versus x is the same using b = 9/2 or 5, the ratio of B/A is plotted in the inset of Fig. 5 using b = 5. Also plotted in the same inset is the ρ_0/A ratio, by the open squares. The x dependence of ρ_0 associated with the residual or disorder scattering process is only slightly higher than that of the AT^a term. From the above analysis for the various scattering processes, the BT^b term is affected most profoundly by the presence of the LCMO/YSZ BL layer, indicating that the BL-induced strain has a strong effect on the electron-phonon coupling strength.

The temperature dependent TEP, $S(T)$, was measured with the series of LCMO/YSZ samples by the home-made insert-probe using the dc differential technique. The electrical contacts were made by the cold-pressed indium. The sample was installed across two temperature platforms. One was regulated at temperature T, while the

other controlled to vary within $T + \Delta T$. A continuous voltage output, ΔV, taken by Keithley 2010 multimeter was recorded with the corresponding ΔT, typically a few tenths of a kelvin, changing slowly. The slope of the linear relation between ΔV and ΔT, with the correction of the contribution from the Cu leads, would give the measured TEP of the sample. Abrupt TEP jumps occur during the magnetic phase transition for the x > 0 % samples, but not for the sample with x = 0 %, see Fig. 6. This demonstrates clearly a strong correlation of the jumps with the existence of the BL, and was interpreted as due to the magnetic inhomogeneity induced by the BL strain[15]. Similar TEP jump with the magneto-TEP effect has been observed in the thin film CMR manganites also[18,19]. The substrate strain unavoidably caused the magnetic inhomogeneity in the sample. Under the applied magnetic field, the inhomogeneous magnetic component has been reduced. The TEP jump was therefore suppressed to show the magneto-TEP effect.

IV. DISCUSSION

The non-magnetic, insulating YSZ component intermixing in the LCMO causes variations in the magnetic and transport properties of the manganites. Most of the interesting features in the physical properties under current investigations are strongly correlated with the LCMO/YSZ BL. Several effects would be introduced on the samples by the existence of the BL. However, only a leading one is accounted for the observed x dependence. The strain induced by the BL would be the major factor identified in the present work.

Usually, the effect of strain on the physical properties of the manganites, especially on the T_C variations, is studied with the films. However, for thickness under a few hundred nanometers, the finite size confinement effect would become important to superimpose on the effect of strain. With the substrate strain, the interface magnetic inhomogeneity has been directly observed by the techniques of NMR[6] or X-ray photoemission spectroscopy[5]. Nonetheless, for these films, the finite size effect seems to be the leading factors in the depression of T_C, dominating the effect of strain under discussion. Fig. 7 displays the shift of T_C versus film thickness, d, summarized from many of the previous experiments for various thin films grown on different substrates[6,10,13,20–25]. The results follows very well the law of finite size confinement[26,27], $|T_C(\infty) - T_C(d)|/T_C(\infty) = (\xi_0/d)^\lambda$ with $\lambda = 1$ in consistent with the result from the mean field theory[8], where $\xi_0 = 6$ nm is the correlation length at T = 0 K, $T_C(d)$ is the transition temperature for a film of thickness, d, and $T_C(\infty)$ is that for the corresponding bulk samples. Note that the dispersion of the data points in Fig. 7 indicates that the effect of the substrate strain and the crystallinity of the films superimposed on top of the confinement effect are non-negligible. This is reasonable since these points are summarized from various experiments performed by different laboratories. The above result indicates that the finite size effect is the leading factor for the suppression of T_C with the thin film samples at a thickness less than a few hundred nanometers, even with the obvious coexistence of the substrate strain often suggested as the solely factor.

For an LCMO cluster enclosed by the YSZ component at the small YSZ fraction, x $\leq$ 4.5 %, T_C drops dramatically with the increasing x. In this region, the cluster size is on the order of several tens of micrometers. This is simply too large for the finite size confinement effect to occur according to the analysis for the thin films. For the YSZ serving as a non-magnetic separation between the LCMO phase, the reduction in the effective magnetic coupling is unlikely the major factor for the x dependence of the T_C depression either. This effect would more or less level off at a layer thickness of a few nm according to the previous experiment[28]. In the present work, the non-magnetic YSZ layer is at least 10 nm in thickness, reaching the region of saturation for such an effect. The effect of intergranular magnetic tunnelling coupling, which is beyond the DE mechanism, is unlikely the major factor either responsible for the observed properties. In this case, the depression of T_C is less than 5 % with T_P lower than T_C by a temperature depending on the extent of the intergranular coupling strength.[12,13,29–32]. The main features of the present results, see Fig. 2, do not fit the description above since T_C is depressed by more than 20 % with the varying x and T_P follows it closely, see Fig. 2. Furthermore, the insulating YSZ layer with a thickness of more than 10 nm is too thick for the electrical current to tunnel through at LT to show metallic property.

In the polycrystalline LCMO/YSZ composite system, the LCMO cluster is larger than 10 μm. The ratio of the boundary strained layer over the volume depends on the thickness of the strained layer. It is possible for the spatial relaxation of an interfacial strain to extend over a distance of 1 μm[33], and results in a non-negligible volume fraction of the boundary strained layer in the bulk LCMO component. According to the previous reports, T_C would be seriously depressed by the biaxial strain resulting from the substrate lattice mismatch. Merely 1 % of the biaxial strain would cause an order of 10 % variation in T_C[35], as demonstrated by the experiment of ultrasound spectroscopy[36]. Yet, such a low level of strain would go undetected by the usual experimental techniques such as the XRD analysis. The magnetic anisotropy or inhomogeneity caused by the strain would explain the depression of T_C, and the corresponding broadening of the magnetic transition, ΔT.

In the analysis of $\rho(T)$ at $T < T_C$, the residual term, ρ_0, and the AT^a term exhibit much less structure dependence than the BT^b term. This is a strong evidence supporting that the electron-phonon coupling strength is modified by the existence of the BL. Since the Jahn-Teller (J-T) phonon mode depends strongly on the biax-

ial strain of the lattice[35], it is reasonable to infer that the x dependence of the BT^b term is caused by the biaxial strain, which affects the magnetic transition, T_C as well.

The strong correlation of the TEP jump during the magnetic transition with the presence of the BL is interpreted as of magnetic origin[15], and can be reasonably explained by the magnetic inhomogeneity induced by the strain. At LT, $S(T)$ shows a typical metallic behavior with a small absolute value. As the temperature increases toward the HT region, the fraction of the PM component having the semiconducting property increases. For the x = 0 sample, the change in the PM fraction relative to the FM one is smooth, showing a smooth transition in $S(T)$. On the other hand, the introduction of the BL with the x > 0 samples would cause an extra contribution from the inhomogeneous magnetism, resulting in an abrupt deviation of $S(T)$ from the metallic region. Interestingly, in the previou work on the series of samples with constant valence, $Pr_{0.7}Ca_{0.3-x}Sr_xMnO_3$[34], the temperature-dependent TEP behavior has been demonstrated to correlate strongly with the magnetic transition. Especially, a TEP jump begins at the temperature near the ferromagnetic-antiferromagnetic (AF) transition as shown in Fig.4 by Hejtmanek *et al*[34]. According to the present picture in explaining the TEP behavior, the occurrence of the AF component within the FM matrix is responsible for the abrupt jump of the TEP. A noteworthy point, however, is that the cause of the inhomogeneous distribution of the magnetism for the $Pr_{0.7}Ca_{0.3-x}Sr_xMnO_3$ samples is attributed to the FM-AF transition, quite different from the existence of the BL-induced strain in the presence work.

V. CONCLUSION

In conclusion, the YSZ component in the LCMO/YSZ composite materials induces a large effect on the various physical properties such as the variations of T_C and T_P, the broadening of magnetic transition, the pronounced TEP jump during the magnetic transition, and the resistivity variation in the LT FM phase, *etc.*. The BL-induced strain plays a crucial role in the explanation of the observed properties. In this respect, the effect of strain is not only important in the manganite film already reported by some of the recent works, but also has a profound effect in the bulk sample, as demonstrated by the present work.

VI. ACKNOWLEDGEMENT

We are grateful to Prof. Songliu Yuan of the Department of Physics, Huazhong University of Science and Technology, Wuhan, China, for providing us with the samples and for the helpful discussions. One of the authors, C.P. Chen, would also like to appreciate Prof. Tong-han Lin of the Department of Physics, Peking University, Beijing, China, for some of the points raised and the fruitful discussions.

---

* e-mail address : cpchen@pku.edu.cn, TEL : +86-10-62751751

[1] C. Zener, Phys. Rev. **82**, 403 (1951)
[2] P. Anderson and H. Hasegawa, Phys. Rev. **100**, 675 (1955)
[3] J. B. Goodenough, Phys. Rev. **100**, 564 (1955)
[4] P. G. de Gennes, Phys. Rev. **118**, 141 (1960)
[5] Hani Dulli, E.W. Plummer, P.A. Dowben, Jaewu Choi, and S.-H. Liou, Appl. Phys. Lett. **77**, 570 (2000)
[6] M. Bibes, Ll. Balcells, S. Valencia, J. Fontcuberta, M. Wojcik, E. Jedryka, and S. Nadolski, Phys. Rev. Lett. **87**, 67210 (2001)
[7] M. Bibes, Ll. Balcells, J. Foncuberta, M. Wojcik, S. Nadolski, and E. Jedryka, Appl. Phys. Lett. **82**, 928 (2003)
[8] Renjun Zhang, Roy F. Willis, Phys. Rev. Lett. **86**, 2665 (2001)
[9] M. Ziese, H.C. Semmelhack, K.H. Han, S.P. Sena, and H.J. Blythe, Appl. Phys. Lett. **91**, 9930 (2002)
[10] A. de Andres, J. Rubio, G. Castro, S. Taboada, J.L. Martinez, J.M. Colino Appl. Phys. Lett. **83**, 713 (2003)
[11] S. L. Yuan, Z. C. Xia, S. Liu, Z. Y. Li, G. Peng, J. Tang, G. H. Zhang, L. J. Zhang, W. Feng, and C. S. Xiong, Chin. Phys. Lett. **19**, 1168 (2002)
[12] R.D. Sanchez, J. Rivas, C. Vazquez-Vazquez, A. Lopez-Qintela, M.T. Causa, M. Tovar, and S. Oseroff, Appl. Phys. Lett. **68**, 134 (1996)
[13] A. Gupta, G.Q. Gong, G. Xiao, P.R. Duncombe, P. Lecoeur, P. Trouilloud, Y.Y. Wang, V.P. Dravid, and J.Z. Sun, Phys. Rev. B **54**, R15629 (1996)
[14] F.M. Araujo-Moreira, M. Rajeswari, A. Goyal, K. Ghosh, V. Smolyaninova, T. Venkatesan, C.J. Lobb, and R.L. Greene, Appl. Phys. Lett. **73**, 3456 (1998)
[15] W. Liu, J. Zhao, C.P. Chen, S.S. Yan, Z.C. Xia, and S. Liu, J. Appl. Phys. **94**, 7206 (2003)
[16] J.A. Mydosh, Chapter 3 in "Spin glass, an experimental introduction", (Taylor & Francis, 1993)
[17] Kenn Kubo and Nagao Ohata, J. Phys. Soc. Japan **33**, 21 (1972)
[18] M. Jaime, M.B. Salamon, K. Pettit, M. Rubinstein, R. E. Treece, J. S. Horwitz, and D. B. Chrisey, Appl. Phys. Lett. **68**, 1576 (1996)
[19] M. Jaime, P. Lin, S. H. Chun, M. B. Salamon, P. Dorsey, and M. Rubinstein,Phys. Rev. B **60**, 1028 (1999)
[20] M. Bibes, S. Valencia, Ll. Balcells, B. Martinez, J. Fontcuberta, M. Wojcik, S. Nadolski, and E. Jedryka, Phys. Rev. B **66**, 134416 (2002)
[21] G. Campillo, A. Berger, J. Osorio, J.E. Pearson, S.D. Bader, E. Baca, and P. Prieto, J. Mag. Mag. Mater. **237**, 61 (2001)
[22] G.J. Snyder, R. Hiskes, S. DiCarolis, M.R. Beasley, and T.H. Geballe, Phys. Rev. B **53**, 14434 (1996)
[23] H. Huhtinen, R. Laiho, K.G. Lisunov, V.N. Stamov, and

V.S. Zakhvalinskii, J. Mag. Mag. Mater. **238**, 160 (2002)
[24] G.C. Xiong, B. Zhang, S.C. Wu, Z.X. Lu, J.F. Kang, G.J. Lian, and D.S. Dai, Solid State Commun. **97** 17 (1996)
[25] R.A. Rao, D. Lavric, T.K. Nath, C.B. Eom, L. Wu, and F. Tsui, Appl. Phys. Lett. **73**, 3294 (1998)
[26] Michael E. Fisher and Michael N. Barber, Phys. Rev. Lett. **28**, 1516 (1972)
[27] J.G. Brankov, D.M. Danchev, and N.S. Tonchev, Section 5.4 in "Theory of critical phenomena in finite size systems : scaling and quantum effects ", (World Scientific, 2000)
[28] M. Sirena, N. Habercorn, L.B. Steren, and J. Guimpel, J. Appl. Phys. **93**, 6177 (2003)
[29] R. Mahesh, R. Mahendrian, A.K. Raychaudhuri, and C.N.R. Rao, Appl. Phys. Lett. **68**, 2291 (1996)
[30] R. Mahendrian, R. Mahesh, A.K. Raychaudhuri, and C.N.R. Rao, Solid State commun. **99**, 149 (1996)
[31] H.Y. Hwang, S.-W. Cheong, N.P. Ong, and B. Batlogg, Phys. Rev. Lett. **77**, 2041 (1996)
[32] S. L. Yuan, Z. C. Xia, L. Liu, W. Chen, L.F. Zhao, J. Tang, G.H. Zhang, L.J. Zhang, H. Cao, W. Feng, Y. Tian, L.Y. Niu, and S. Liu, Phys. Rev. B **68**, 184423 (2003)
[33] Yeong-Ah Soh, P.G. Evans, Z. Cai, B. Lai, C.-Y. Kim, G. Aeppli, N.D. Mathur, M.G. Blamire, and E.D. Isaacs, J. Appl. Phys. **91**, 7742 (2002)
[34] J. Hejtmanek, Z. Jirak, D. Sedmidubsky, A. Maignan, Ch. Simon, V. Caignaert, C. Martin, and B. Raveau, Phys. Rev. B **54**, 11947 (1996)
[35] A.J. Millis, T. Darling, and A. Migliori, J. Appl. Phys. **83**, 1588 (1998)
[36] T.W. Darling, A. Migliori, E.G. Moshopoulou, Stuart A. Trugman, J.J. Neumeier, J.L. Sarrao, A.R. Bishop, and J.D. Thompson, Phys. Rev. B **57**, 5093 (1998)

FIG. 1. XRD spectra for the series of samples, (1-x)LCMO/(x)YSZ. The XRD was performed by a Philip x' pert diffractometer using the Cu K_α line (1.54056 $\AA$). At x $\leq$ 4.5 %, only the LCMO phase is observed. The YSZ phase shows up at x $>$ 4.5 %.

FIG. 2. x dependence of Curie temperatures, $T_C(dc)$ by dc magnetization and $T_C(ac)$ by ac susceptibility, metal-insulator transition temperature, T_P, and magnetic transition width in temperature, ΔT.

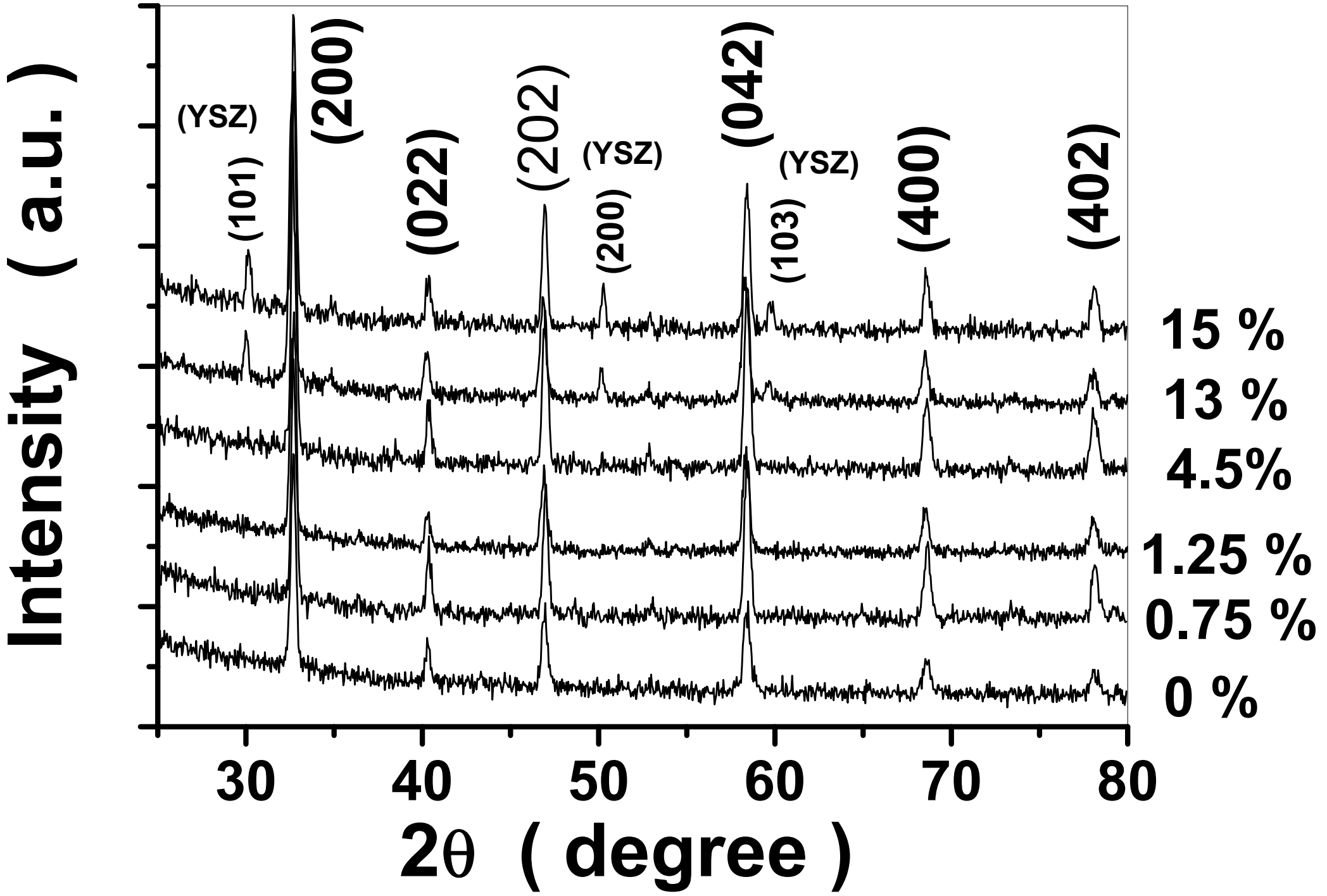
FIG. 3. Out of phase component of magnetic susceptibility, χ'', versus temperature, T, for samples with various YSZ concentration, x. The inset shows the x dependence of the two dissipation characteristic temperatures, T_{DH}, corresponding to the critical fluctuation around the ferromagnetic transition and, T_{DL}, associated with the disorder spin state on the polycrystalline grain surface.

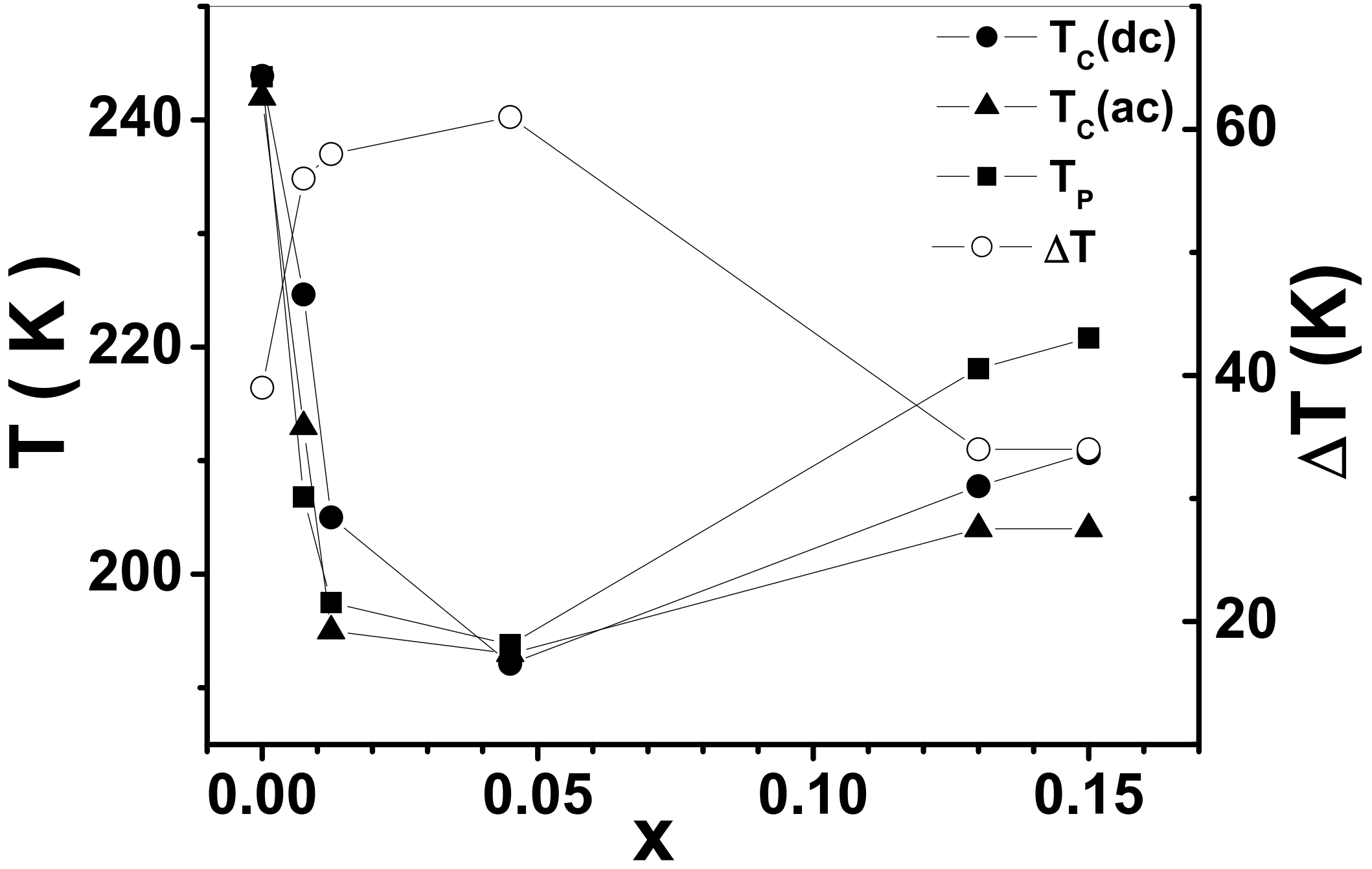
FIG. 4. FC-ZFC dc magnetization. M_m is the maximum magnetization occurring near the freezing temperature. The solid symbols are for the FC results, and the open ones are for the ZFC branches.

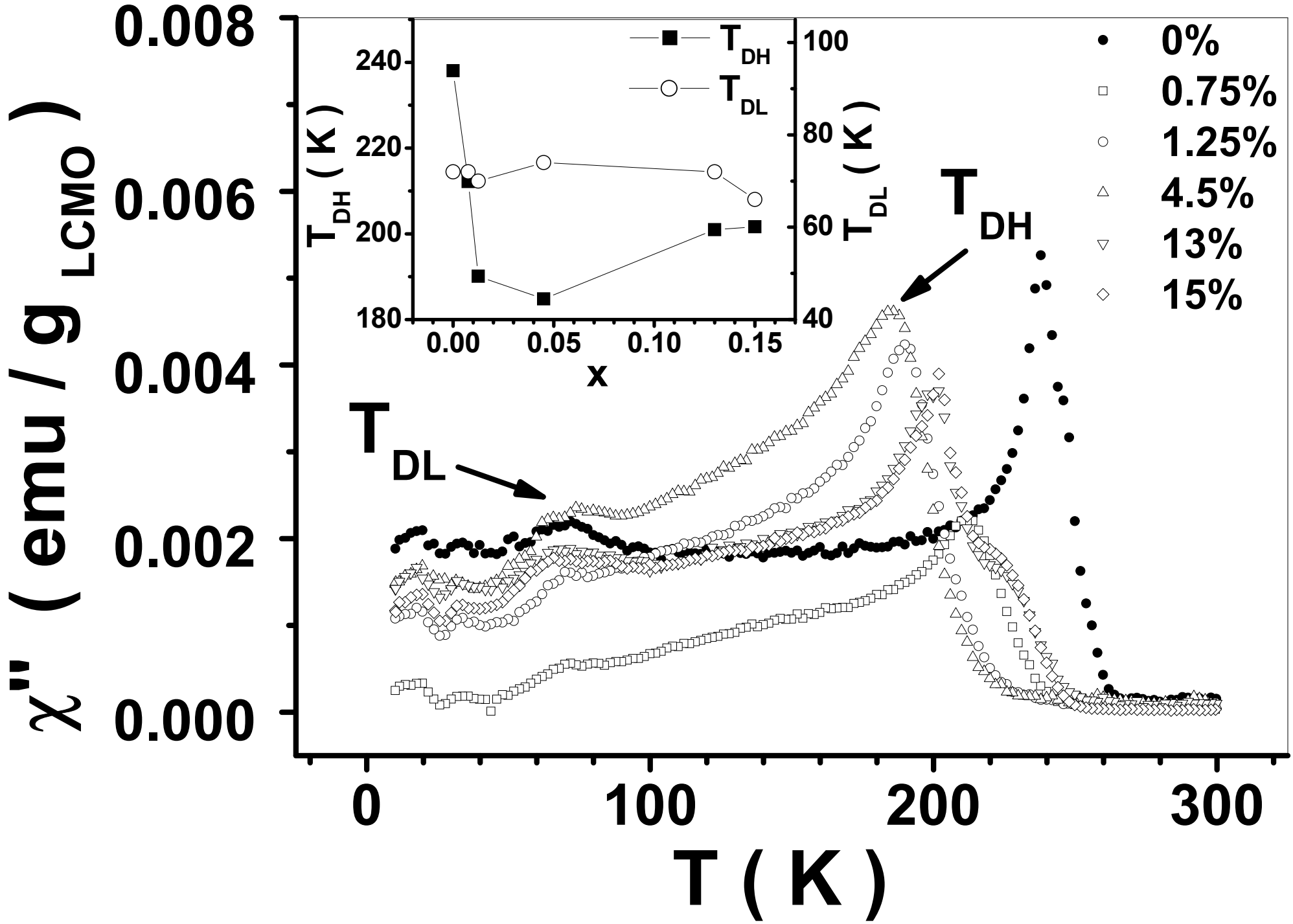
FIG. 5. x dependence of the scattering processes of electrical transport at $T < T_C$. The resistivity is fitted by the equation, $\rho(T) = \rho_0 + AT^2 + BT^5$ to obtain ρ_0, A, and B. The fitting range in temperature is $T < 0.8T_C$. The solid circles in the inset represent the ratio of B/A, which show variation with more than an order of magnitude.

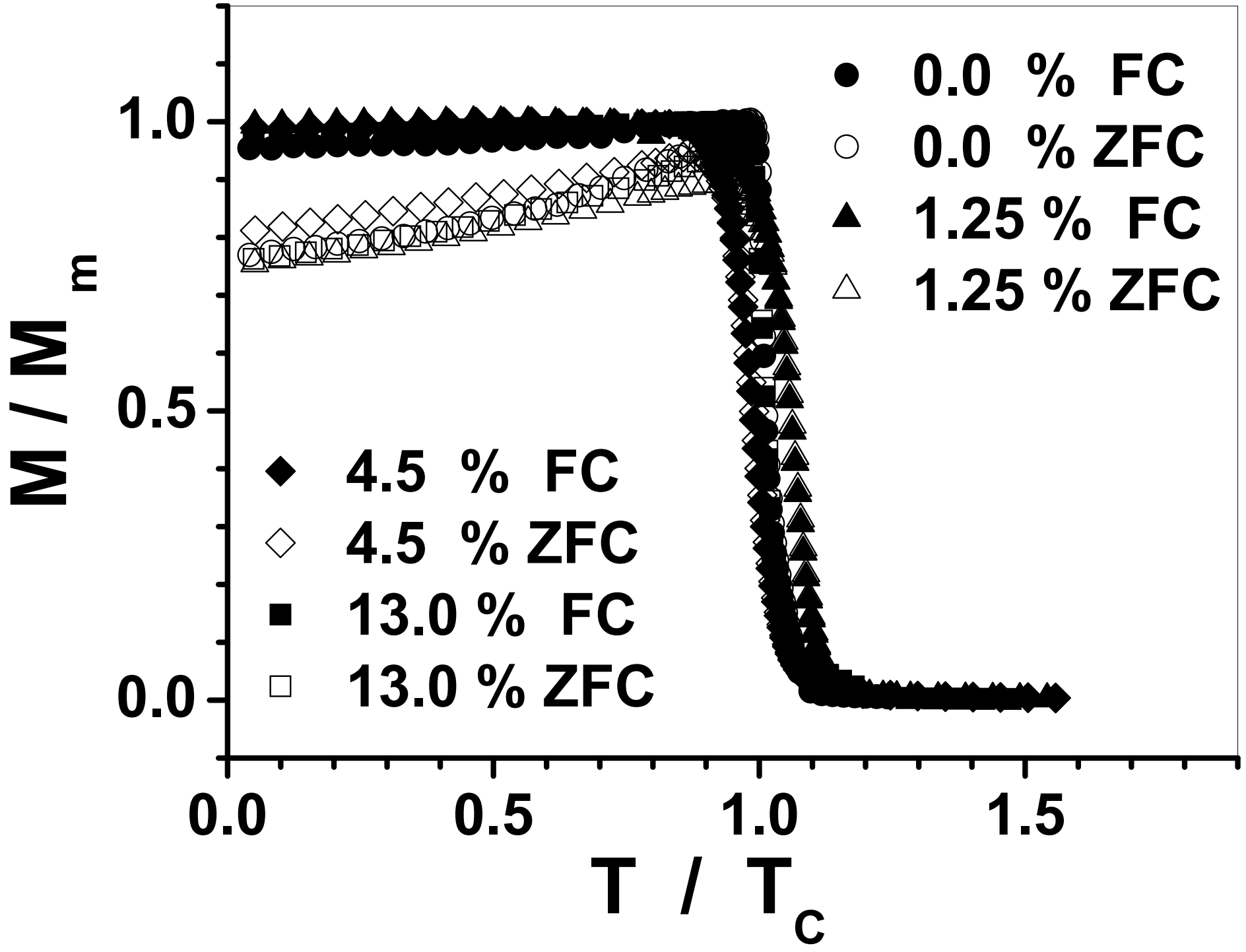
FIG. 6. Temperature dependent TEP of the samples with various YSZ fraction, x. The solid circle is for x = 0%, while the open ones for samples with x $>$ 0.

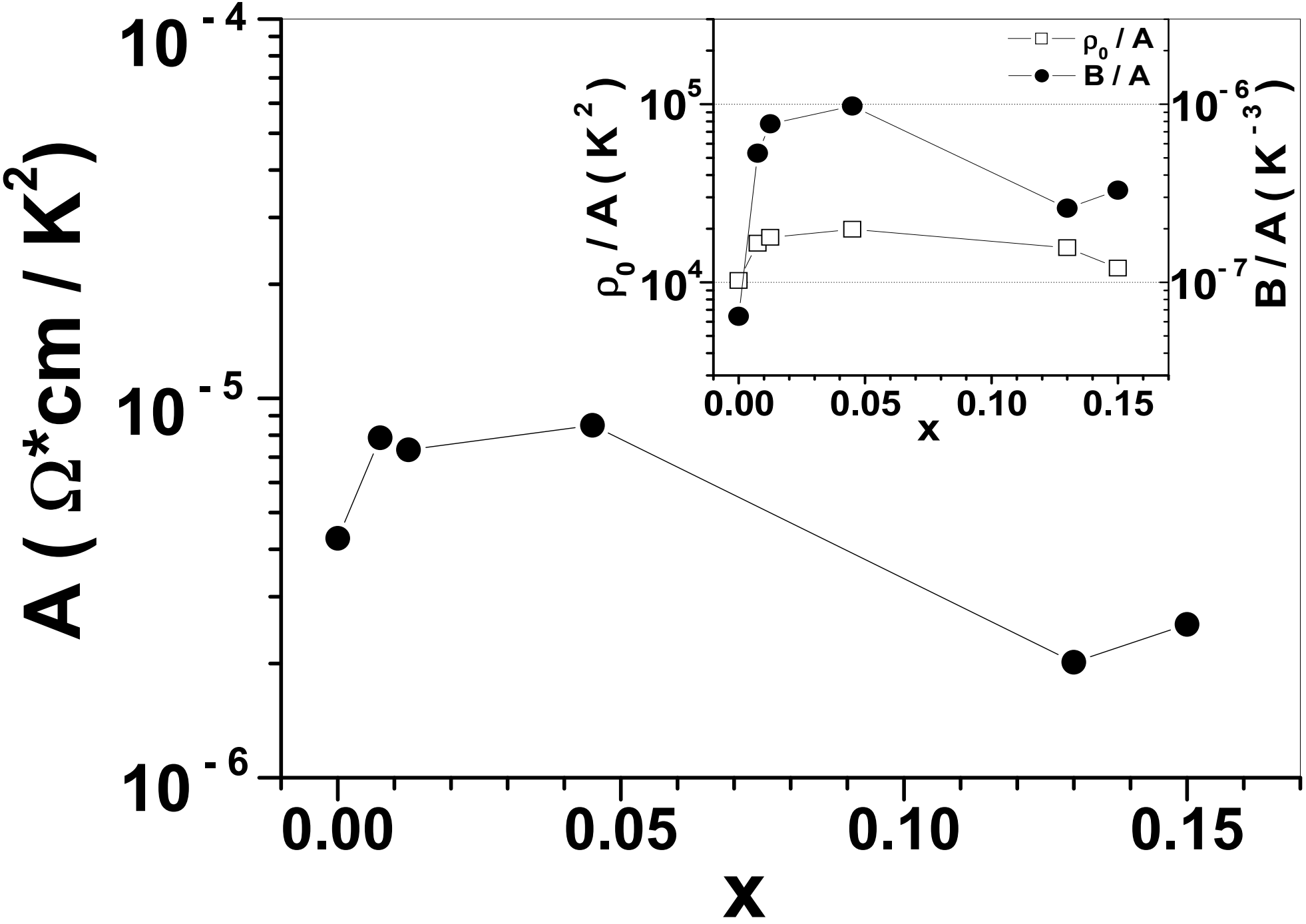
FIG. 7. Finite size confinement effect on the shift of magnetic transition temperature according to the equation, $|T_C(\infty) - T_C(d)|/T_C(\infty) = (\xi_0/d)^\lambda$, for various thin manganite films on different substrates. The solid line is calculated using the above equation with $\lambda = 1$ and $\xi_0 = 6$ nm. The manganite films include, $La_{2/3}Ca_{1/3}MnO_3$ (LCMO), $La_{2/3}Sr_{1/3}MnO_3$ (LSMO), $Pr_{2/3}Sr_{1/3}MnO_3$ (PSMO), and $La_{0.8}Ca_{0.2}MnO_3$, while the substrates are $SrTiO_3$ (STO), $LaAlO_3$ (LAO), and $NdGaO_3$ (NGO). These results are summarized from the experiments, (a)[20], (b)[6], (c)[10], (d)[13], (e)[21], (f)[22], (g)[23], (h)[24], (i)[25].

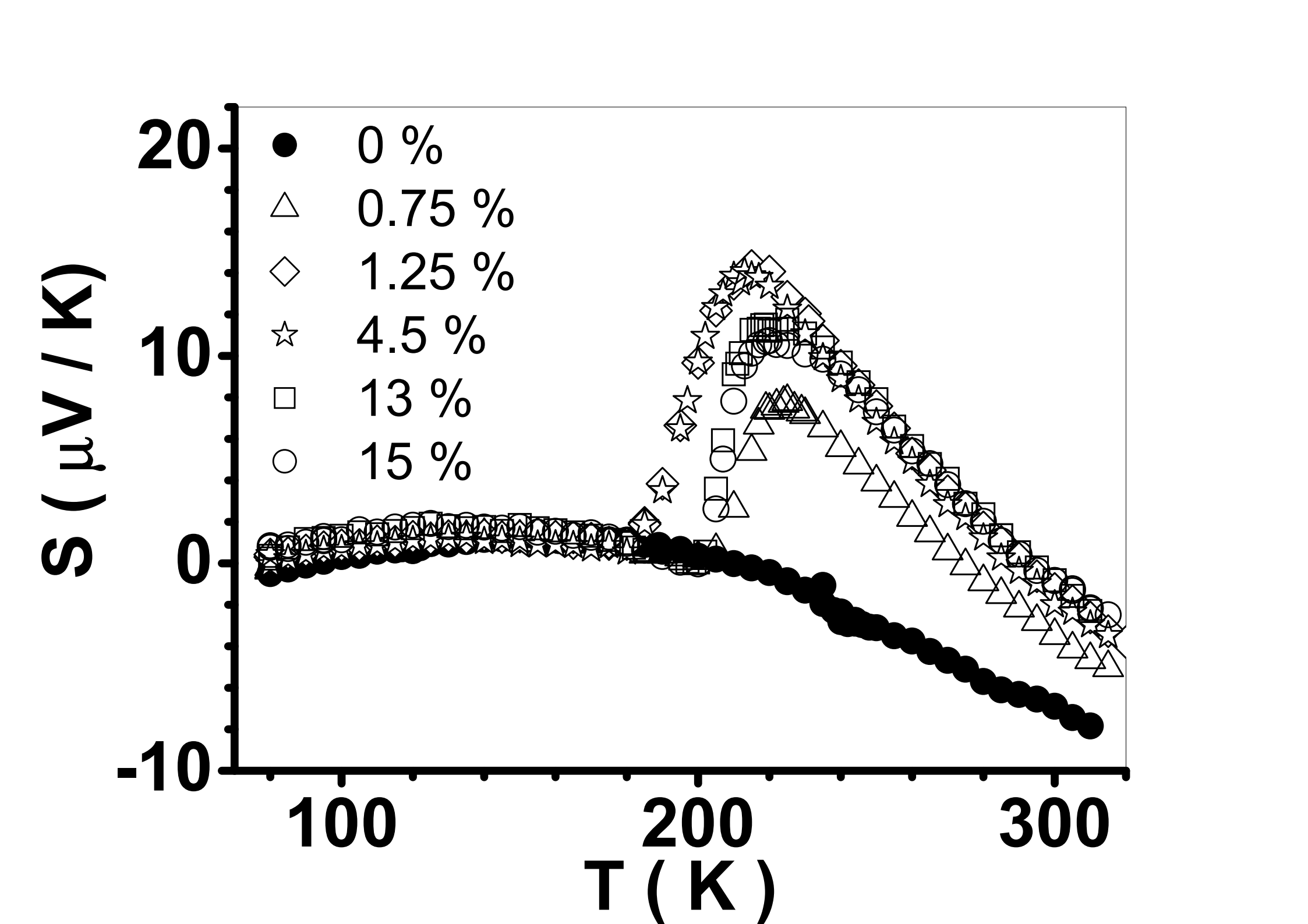

Intensity (a.u.)
(YSZ)
(101)
(200)
(022)
(202)
(YSZ)
(200)
(042)
(YSZ)
(103)
(400)
(402)
15 %
13 %
4.5%
1.25 %
0.75 %
0 %
30
40
50
60
70
80
2θ (degree)

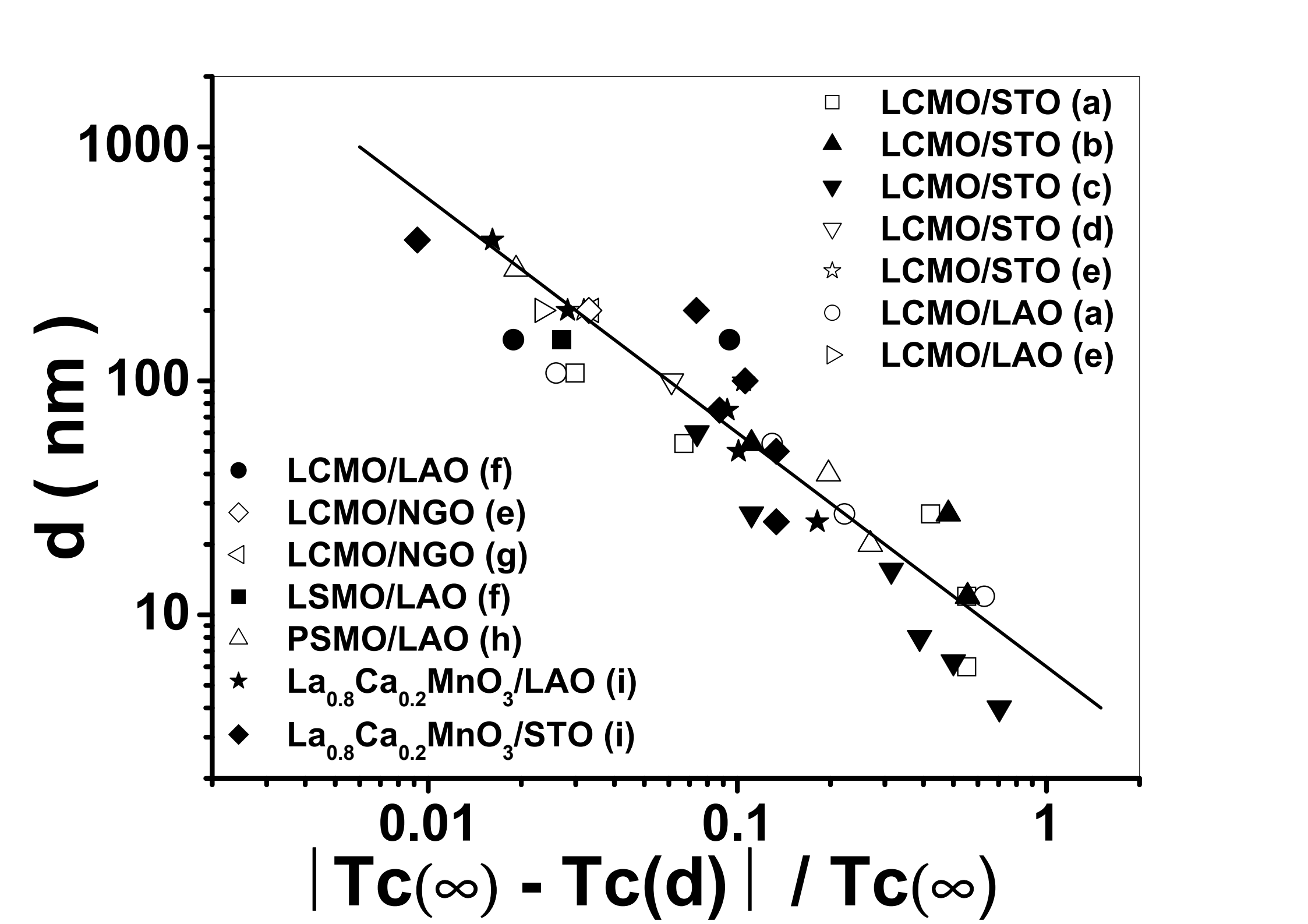

T (K)
240
220
200
0.00
0.05
0.10
0.15
X
60
40
20
ΔT (K)
T_c(dc)
T_c(ac)
T_P
ΔT


χ'' (emu / g LCMO)
0.008
0.006
0.004
0.002
0.000
0
100
200
300
T (K)
T DH
T DL
0%
0.75%
1.25%
4.5%
13%
15%
T DH (K)
T DL (K)
x
240
220
200
180
100
80
60
40
0.00
0.05
0.10
0.15


M / M m
1.0
0.5
0.0
0.0
0.5
1.0
1.5
T / T C
0.0 % FC
0.0 % ZFC
1.25 % FC
1.25 % ZFC
4.5 % FC
4.5 % ZFC
13.0 % FC
13.0 % ZFC


A (Ω*cm / K2)
10 - 4
10 - 5
10 - 6
0.00
0.05
0.10
0.15
X
ρ0 / A
B / A
ρ0 / A (K2)
B / A (K-3)
10 5
10 4
10 - 6
10 - 7
0.00
0.05
0.10
0.15
x


20
10
0
-10
S (μV / K)
100
200
300
T (K)
0 %
0.75 %
1.25 %
4.5 %
13 %
15 %


1000
100
10
d (nm)
0.01
0.1
1
| Tc(∞) - Tc(d) | / Tc(∞)
LCMO/STO (a)
LCMO/STO (b)
LCMO/STO (c)
LCMO/STO (d)
LCMO/STO (e)
LCMO/LAO (a)
LCMO/LAO (e)
LCMO/LAO (f)
LCMO/NGO (e)
LCMO/NGO (g)
LSMO/LAO (f)
PSMO/LAO (h)
La0.8Ca0.2MnO3/LAO (i)
La0.8Ca0.2MnO3/STO (i)